JSST
Journal of Space Science and Technology

P-ISSN: 2008-4560
E-ISSN: 2423-4516

Journal of Space Science and Technology

Vol. 18, No. 4, pp. 22-31, 2025
https://doi.org/10.22034/jsst.2025.1519
Journal Homepage: https://www.jsstpub.com

Original Research Paper

Evaluating Optimal Ultrasound to Deform the Blood Clot in a Vessel for Astronauts' Health

Ramin Kamali Moghadam[1], Mahmoud Najafi[2], Masoomeh Azadegan[3], and Nasrin Sahranavardfard[4]

1. Aerospace Research Institute, Ministry of Science, Research and Technology, Tehran, Iran
2. Department of Mathematical Sciences, Kent State University, Ohio, USA
3. Department of Electrical Engineering, Khatam University, Tehran, Iran
4. Department of Engineering, University of Perugia, Perugia, Italy

ARTICLE INFO

Article History:

Received 11 January, 2025
Revised 2 August, 2025
Accepted 9 August, 2025
Available 2 Online September, 2025

Keywords:

Bubble dynamic
Ultrasound control
3D CFD
Blood clot deformation
Astronauts health

ABSTRACT

Formation of a blood clot in the astronaut's veins in space may have dangerous consequences. In the absence of gravity, body fluids shift from the legs to the upper body and the head. This shift affects the flow of blood through the vessels in the head. Removing the blood clot in the vessels in space may help astronauts' health. Although using the medicine to remove the blood clot in the vein, it can be applied only for a very small size. When the blood clot is large, using the ultrasonic waves with the creation of small bubbles may be a useful method to remove the blood clots in the veins. The goal of the present paper is to gain an optimal intensity of ultrasound to achieve the required pressure field generated by the collapsing bubble in blood to deform blood clots. The collapse pressure within the bubble has been calculated using the Rayleigh–Plesset (RP) equation. Moreover, a coupling simulation of the flow and clot structure is performed using the full Navier-Stokes equations, which govern the blood domain, and linearized discrete equations for the clot medium to calculate the desired bubble collapsing pressure necessary to deform the clots, which has immense importance in medical applications. Simulation results are presented to show the effectiveness of the proposed method.

* Corresponding Author's E-mail: rkamali@ari.ac.ir

How to Cite this Article:
R. Kamali Moghadam, M. Najafi, M. Azadegan, and N. Sahranavardfard, "Evaluating optimal ultrasound to deform the blood clot in a vessel for astronauts health," *Journal of Space Science and Technology*, Vol. 18, No. 4, pp. 22-31, 2025, https://doi.org/10.22034/jsst.2025.1519.

1. INTRODUCTION

Blood clots that create in arteries feeding the heart and brain are the major cause of heart attacks and deep vein thrombosis, i.e., pelvic area, clots in the legs, and upper extremities [1]. The pieces of the clot may fracture and move to an artery in the lungs, resulting in an acute pulmonary embolism. As blood clots have a complex microscopic structure, additional analysis is needed. Among various blood clot components, optical microscopy has been found to be convenient for studying blood clot structure and interactions [2]. In this study, the blood clot is considered as a homogeneous continuous medium in a vessel connected to a pulmonary artery.

Thrombolysis is the dissolution of a blood clot created in blood vessels using medication that is used in stroke and severe venous thromboembolism. Thrombolytic therapy is a treatment that breaks up dangerous blood clots in blood vessels, improves blood flow, and prevents tissue and organ damage. Thrombolysis may involve injecting a clot-busting drug through an intravenous line or a long catheter that delivers the drug straight to the location of the blockage. It may also involve using a long catheter with a mechanical device at the tip to remove or physically break up the clot [1]. Thrombolytic therapy, if the blood clot is determined to be life-threatening, and if started as soon as possible, ideally within 1 to 2 hours of symptoms of heart attack, stroke, or pulmonary embolism, could be one of the choices [1,3-5]. Despite a long history of research into the diagnosis and prognosis of pulmonary embolism, the disease remains a cause of high mortality, with an untreated mortality rate of 15% in normotensive patients and 15% in patients with cardiogenic shock, up to 58% [6]. Thrombolytic therapy is valuable in treating considerable pulmonary embolism [7] and acute/subacute arterial thrombosis [8].

Cavitation, the formation of bubbles in a liquid under an ultrasonic field, can be used as an efficient, non-invasive thrombolysis technique. However, bubble formation refers to both the formation of new bubbles and the expansion of existing microbubbles [9]. As cavitation bubbles grow and collapse, they produce various physical effects such as microjets, shear forces, shock waves, etc [10]. The physical effects of ultrasound can be applied to a variety of subjects, including physics, chemistry, food technology, and engineering [11,12]. Moreover, ultrasound is useful in surgical, therapeutic, and diagnostic medical applications [13,14]. Cavitation has an important role in various medical applications [13]. Researches on the collapse of cavitation bubbles are widely documented in the literature. Cavitation bubbles can be explained by the oscillatory dynamics, the very high temperature and pressure that occur at the moment of collapse. When a cavitation bubble collapses, it creates thousands of atmospheres of pressure within the bubble for just a few microseconds [15]. These characteristic parameters can be determined both experimentally and theoretically for a single bubble [16-20]. Study efforts have focused on using cavitation as an efficient, non-invasive thrombolysis technique[21-22]. Most of the previous research was based on experimental results, and the minimum pressure required to break down a blood clot has not yet been theoretically determined.

The acoustic pressure and mechanical index have been modeled in [23] to calculate the optimal intensities and distances from the transducer in cylindrical coordinates and validate the results experimentally. Authors in [24] have numerically performed the coupling of blood and clot simulation according to the different initial pressures generated by bubble collapse to find the minimum pressure required to pass the yield stress and consequently clot deformation. Also, the RP equation has been used to obtain the bubble radius and calculate the collapse pressure within the bubble. Finally, the ultrasound frequency has been appropriately selected to achieve the desired collapse pressure.

This paper is an improved and extended version of [24]. The dimensions of blood vessels and blood clots have been chosen in a way that is close to reality, and the work of their practical implementation is also underway. Also, according to [25], the appropriate frequency was selected, and based on that, the optimal distance from the transducer was determined based on [23]. Finally, the appropriate intensity level needed for detachment of the clot has been calculated and applied through cavitation using an ultrasound signal. When finding the minimum required intensity and pressure consequently, blood flow is first simulated in the vein using Ansys/Fluent software. Then, the effects of a pressure pulse on the clot caused by a bubble collapse are investigated using structural and dynamical analysis. Finally, the maximum amount of stress obtained on the clot is

compared with the clot yield stress to find the minimum amount of pressure required. To study the effects of a pressure pulse, the proposed models simulated a selected physical domain of a clot in a vein using a 3D CFD simulation.

This method provides proper treatment planning in vitro and in vivo by estimating the cavitation phenomenon and its effect on the clot.

2. CAVITATION BUBBLE DYNAMICS

The use of control algorithms for stability analysis and control of a single spherical bubble was presented for the first time in [26]. In this section, we analyzed bubble dynamics using simulations. Assuming the initial formation of a bubble, the motion of a single bubble in liquid bulk due to an applied acoustic has been investigated. The RP equation, which is a second-order, nonlinear ordinary differential equation, has been considered to describe single spherical bubble dynamics [27].

$$R\ddot{R}+\frac{3}{2}\dot{R}^2=\frac{1}{\rho}\left(P_0+\frac{2\sigma}{R_0}-P_v\right)\left(\frac{R_0}{R}\right)^{3\gamma} + P_v-\frac{2\sigma}{R}-4\mu\frac{\dot{R}}{R}-P_0-P(t), \quad (1)$$

In the above equation, R is the bubble radius, ρ, σ, μ, and γ are liquid density, liquid surface tension, liquid viscosity, and the ratio of specific heats, respectively. P_0 is atmospheric pressure and P_v is vapor pressure. $P(t)$ represents the additional external pressure applied at the bubble wall. This is modeled as a spatially homogeneous standing sound wave, i.e., $P(t)=-P_a\cos(\omega t)$, where P_a is ambient pressure, and ω is a fixed frequency. Since the intensity of the ultrasound can be adjusted in vitro, we use the following equation to calculate the pressure.

$$\boldsymbol{I_0=\frac{P_a^2}{2\rho v_m}},\quad \boldsymbol{I=I_0e^{\acute{\mu}x}} \quad (2)$$

In which I_0 is the ultrasound intensity, v_m is the velocity of the sound wave, $\acute{\mu}$ is the absorption coefficient, x is the distance from the transducer, and I is the ultrasound intensity at distance x. Also, R_0 is the radius of the unforced bubble, and dots over a term denote derivatives with respect to time, t.

3. PRESSURE DUE TO BUBBLE COLLAPSE

In the rarefaction cycle of the acoustic wave, the bubble radius reaches its maximum value and collapses violently. As a result of the collapse of the bubbles, substantial amounts of pressure and heat are generated in the liquid bulk around the bubble instantaneously. As the collapse time is on the order of microseconds, the heat cannot escape from the bubble, and the bubble's collapse can be considered adiabatic. Bubble pressure is an important feature of a cavitation bubble. Assuming adiabatic compression, the collapse pressure inside the bubble can be calculated with Eq. (3) [17]:

$$\boldsymbol{P_{collapse}=\frac{R_0^3P_0}{\frac{4}{3}R^3(t)}} \quad (3)$$

The nonlinear model Eq. (1) is simulated using the parameters given in Table I, which are common values for studying a bubble collapse in blood [28]. The driving frequency f and the distance from the transducer are considered the same as the optimal values obtained from [23], which means 1 MHz and 2.5 cm, respectively. We considered four different values for the intensity of the ultrasound, from 0.5 to 2 $^{watt}/_{cm^2}$. The curve of the bubble radius with time for the bubble collapsing in blood is shown in Fig. 1a and Fig. 1b. shows the pressure at the bubble wall as a function of time under different ultrasound intensities.

When the bubble collapses, the potential energy of the enlarged cavity is converted to kinetic energy in the blood. The difference between the pressure outside and inside the bubble is the driving force. During the collapse phase, the bubble is compressed until the pressure inside the bubble is sufficient to balance the forces of contraction. At the collapse point, the collapse is completely arrested; therefore, the bubble begins to rebound. Due to the very rapid change in momentum of the bubble surface, when it reaches its minimum size, extremely high pressure is created, which can lead to deformation of the blood clots.

Table 1. Constant parameters of RP [1].

Parameter	Value	Unit
ρ	1060	$^{kg}/_{m^3}$
σ	0.056	$^{N}/_{m}$
μ	$3*10^{-3}$	$Pa.s$
p_v	4.24×10^3	Pa
p_0	101325	Pa
f	1	$M.Hz.$
R_0	2.5	μm
v_m	1540	$^{m}/_{s}$

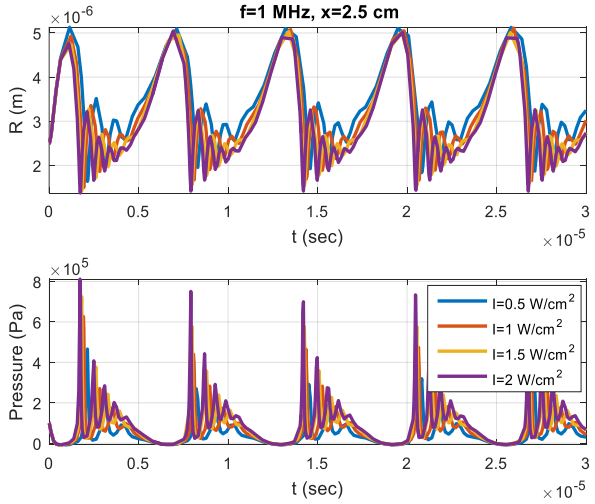

Fig. 1. (A): The curve of the bubble radius with time for bubble collapsing in blood, (B): The pressure at the bubble wall as a function of time; the driving ultrasound frequency is 1 MHz with intensity of 0.5, 1, 1.5, and 2 W/cm^2.

As you can see, the driving ultrasound intensity affects the motion of the bubble wall and consequently the collapse pressure. The collapse pressure for different ultrasound intensity values is shown in Table 2. As seen, the collapse pressure increases with increasing I. The comparison between our numerical results and the experimental results presented in [20] shows that the pressure predicted by Eq. (2) can accurately model the experimentally measured pressure. The necessary pressure to deform blood clots can be achieved by accurately choosing an ultrasound Intensity. In the ensuing sections, the minimum pressure required for breaking down a blood clot is calculated.

Table 2. $P_{collapse}$, for various Intensities.

Intensity (W/cm^2)	Collapse Pressure (MPa)
0.5	0.29
1	0.46
1.5	0.58
2	0.75

4. MINIMUM REQUIRED PRESSURE FOR CLOT DETACHMENT

In this section, the goal is to find the minimum required pressure to detach a clot in a vein. For this purpose, a coupling simulation of flow and clot structure is performed. The paper is related to the vessels that are connected to the pulmonary veins, and the clot dimensions are considered due to the vessel dimensions. As shown in Fig. 2, a clot measuring 2 mm in diameter and 20 mm in length is considered in a vein 3 mm in diameter and 60 mm in length. The clot is located 20 mm from the inlet. Using these parameters, the blood and clot are simultaneously simulated as a flow and a solid, repectively. As the flow conditions, in this case, we assume that the blood is a non-Newtonian and viscoelastic material, so it exhibits both viscous and elastic characteristics when undergoing deformation.

The inflow pressure of the vein inlet is specified to calculate the amount of pressure on the clot at various times. Since the clot is considered a solid with a fixed constraint on the vein wall, the blood inlet pressure causes deformations and stresses in the clot. Thus, blood pressure variations on the clot determine the amount of equivalent stress and total deformation.

The inlet pressure is considered the normal blood pressure, which dramatically increases nearly instantaneously due to the bubble collapsing. Rather than simulating the collapsing bubble, the pressure jump resulting from the collapse is considered as the blood inlet pressure. The blood and clot properties are summarized in Tables 3 and 4.

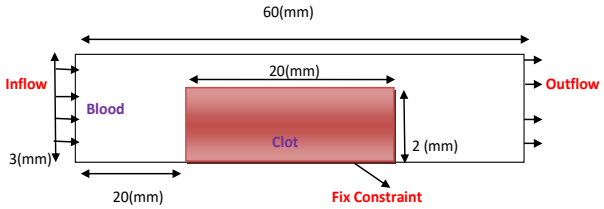

Fig. 2. Problem definition.

Table 3. Blood properties [2].

Dynamic viscosity	Temperature	Density
3e-3 pa.s	310.925 k	1060 kg/m^3

Table 4. Clot properties [2].

Young's module	Poisson's ratio	Density
1.9e6 pa	0.49	5.9e3 kg/m^3

Since blood and clots are considered, respectively, as a flow and a solid, the problem formulation includes two types of governing equations: fluid and structure.

4.1 Flow Governing Equations

The full Navier-Stokes equations govern the flow of a non-Newtonian fluid. The model for clot fragmentation presented here could be further improved by including more advanced fluid-structure interaction combined with biochemical reactions governing dissolution kinetics [29,30]. Although the blood flow in the veins with normal blood pressure is laminar, in thrombolysis, we have a high-amplitude pressure pulse, which raises the velocity and may convert the flow from laminar to turbulent. Consequently, to cover the physics of a pressure pulse, the blood flow is considered to be turbulent. In the present work, the k-ϵ model, one of the most common turbulence models, is used to numerically simulate a complex flow field due to its balance of accuracy, robustness, and computational efficiency. This turbulence model has been extensively tested and validated across a wide range of turbulent flows (e.g., boundary layers and internal flows). The turbulent kinetic energy equation in the k-ϵ method, accurately models the mixing flow near the wall and the wall function use the turbulent kinetic energy (k) to calculate accurate shear stress at the wall. Thus, the k-ϵ model is suitable for the problem with a complex mixing layer near the wall. The compressible RANS equations can be derived by time averaging of the Navier-Stokes equations:

$$\frac{\partial \rho}{\partial t}+\frac{\partial \rho u_i}{\partial x_i}=0 \tag{4}$$

$$\frac{\partial \rho u_i}{\partial t}+\frac{\partial \rho u_i u_j}{\partial x_j}=-\frac{\partial p}{\partial x_i}+\frac{\partial}{\partial x_j}\left[\mu\left(\frac{\partial u_i}{\partial x_j}+\frac{\partial u_j}{\partial x_i}\right)-\rho\overline{u_i'' u_j''}\right] \tag{5}$$

$$\frac{\partial \rho H}{\partial t}-\frac{\partial p}{\partial t}+\frac{\partial \rho H u_j}{\partial x_j}=\frac{\partial}{\partial x_j}(\lambda\frac{\partial T}{\partial x_j}-\rho\overline{Hu_j''})+\frac{\partial}{\partial x_j}\left[u_i\left[\mu\left(\frac{\partial u_i}{\partial x_j}+\frac{\partial u_j}{\partial x_i}\right)-\rho\overline{u_i'' u_j''}\right]\right] \tag{6}$$

where u_i and u_j are the flow velocity components in the x and y directions, ρ is density, p is pressure, μ is viscosity, H is enthalpy, and T is temperature. The Reynolds stress expression, $\rho\widetilde{u_i}\widetilde{u_j}$, is modeled using the eddy viscosity, μ_t. In the k-ϵ turbulent model, the eddy viscosity, is given by $\mu_t = C_\mu \rho \frac{k^2}{\epsilon}$, where the turbulence kinetic energy (k) and the specific rate of dissipation (ϵ) are calculated from two extra transport equations [31]. This allows a two-equation model to account for history effects like convection and diffusion of turbulent energy. Details of the numerical method applied in the present work are available in [32,33].

4.2 FSI Governing Equation

The linearized discrete equations of a structure/solid medium at time t can be expressed as follows:

$$[M]\{\ddot{U}\}+[C]\{U\}+[K]\{U\}=\{F\} \tag{7}$$

where M(u), C(u), and K(u) are the mass, dissipation matrix, and stiffness matrix, respectively, the vector of incremental nodal point displacements is u, and the vector of external forces is F(u), which are applied through the flow. In this paper, the FSI equation is solved using a finite element approach, where a finite element is chosen for each specific problem. The FEM converts a PDE into a system of equations in matrix form. The matrix contribution of each element is calculated and assembled into a global system of equations. In contrast to linear problems, where the solver solves for the displacements and reactions in one step, nonlinear problems need several iterations to solve for the same. The displacement of each node of the structure is calculated from the governing equation. Using that, the strain vector $\{\varepsilon\}$ can be computed from the nodal displacement vector, $\{U\}$ [34].

$$\{\varepsilon\}=[B]\{U\} \tag{8}$$

where $[B]$ is the strain-displacement matrix based on the element-shaped function. Finally, the stress vector, $\{\sigma\}$, is obtained using the strains vector:

$$\{\sigma\}=[D]\{\varepsilon^{el}\} \tag{9}$$

where $[D]$ is the elastic stiffness matrix, and the elastic strain vector, $\{\varepsilon^{el}\}$, is calculated from the total strain vector, $\{\varepsilon\}$ and the thermal strain vector, $\{\varepsilon^{th}\}$:

$$\{\varepsilon^{el}\}=\{\varepsilon\}-\{\varepsilon^{th}\} \tag{10}$$

The von Mises or equivalent stress σ_e is computed from the principal stress components $(\sigma_1, \sigma_2, \sigma_3)$:

$$\sigma_e = \left(\frac{1}{2}[(\sigma_1 - \sigma_2)^2 + (\sigma_2 - \sigma_3)^2 + (\sigma_3 - \sigma_1)^2]\right)^{\frac{1}{2}} \quad (11)$$

4.3 Numerical method

The commercial CFD solver Fluent 15.0 was used to perform the simulations, based on the finite volume approach to solving the governing equations with a segregated solver. The second-order upwind scheme was used for the discretization of the convection terms: energy, turbulent kinetic energy, and turbulent dissipation energy. This scheme ensures, in general and especially for tetrahedral and polyhedral mesh flow domains, satisfactory accuracy, stability, and convergence. The SIMPLE algorithm was used to resolve coupling between the velocity and pressure fields. In the present study, coupled FSI simulation is adopted. Different meshes are generated for the fluid field and the solid field. The case simulation is running until a convergence criterion is reached, i.e., the change in the deflection from iteration to iteration is less than a certain value (10^{-5}). The under-relaxation factors are also considered to be 0.3 and 0.7 for pressure and momentum, respectively.

4.4 Boundary Conditions

In the transient structural analysis, the interior of the clot is considered a fixed support, and the effect of structural damping is included in the structural model. The computational fluid model is created with the side boundaries flush with the ends of the circular vein. The pressure at the inlet is set according to the blood pressure. At the outlet, a pressure-outlet condition is used. A constant inlet temperature of 37 ^{o}C is imposed on the vein inlet. No slip conditions are applied on the surfaces of the vein wall. The single-phase unsteady approach for fluids is adopted in this numerical study.

The pressure pulse caused by the bubble collapse is a time-dependent sine function, which is used for the inlet pressure:

$$P = 2666 + Po \sin\left(\frac{2\pi}{T}t\right) \quad (12)$$

where T is the period of time for the pressure pulse, which is calculated from the simulation of ultrasound bubble formation and collapse, and the flow direction in the inlet boundary is normal to the inlet surface. Unlike systemic blood pressure, which represents the force of the blood moving through the blood vessels in the body, pulmonary blood pressure reflects the pressure the heart exerts to pump blood from the heart through the arteries of the lungs. In other words, it focuses on the pressure of the blood flow in the lungs. Normal pulmonary artery pressure is 8-20 mm Hg at rest. If the pressure in the pulmonary artery is greater than 25 mm Hg at rest or 30 mm Hg during physical activity, it is abnormally high and is called pulmonary hypertension. In this paper, we consider 20 mmHg or 2666 Pa for blood pressure because the investigated artery is connected to a pulmonary vein.

P0 represents the amplitude of the pressure pulse, which is varied by bubble size and collapse. The sample inlet pressure function as an inlet boundary condition is shown in Fig. 3 for an amplitude of P0=1 MPa and a period time of $T=5\times10^{-7}$s. This pressure pulse is applied according to the calculation of the bubble collapse in the previous section. In this section, the pressure is the total pressure of the vein, including the blood pressure and the pressure pulse caused by the bubble collapse.

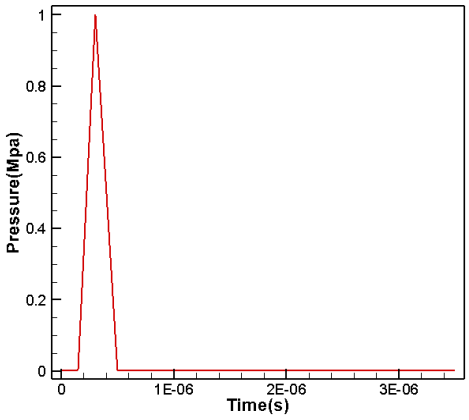

Fig. 3. Inlet pressure pulse (total pressure of the vein, including the blood pressure and the pressure pulse caused by the bubble collapse).

4.5 Mesh Treatment

In order to have an exact numerical simulation that covers the relevant features, good-quality mesh generation is necessary. The tetrahedral elements are used for meshing the entire field. A fine mesh for regions near the wall is needed to have acceptable results. In the present solution, the total number of tetrahedral mesh elements used in all simulations is 13351 for flow. The boundary layer mesh is used near the wall, and grid independence is performed for the pressure drop in the vein as an important parameter in such phenomena. For capturing the ultrasound

physics and frequency of 1 MHz, the CFL=10^ -8 has been considered in all numerical solutions.

A sample of mesh, which is used in the simulations, is presented in Fig. 3.

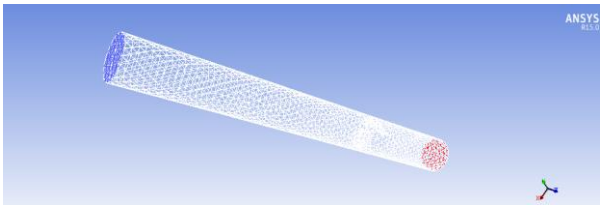

Fig. 4. Mesh generated in the vein for numerical simulation.

5. RESULTS AND DISCUSSIONS

The goal is to control and apply a pressure field generated by the collapsing bubble in blood using ultrasound to fracture blood clots. Firstly, the Rayleigh–Plesset equation has been used to obtain a realistic estimate of the bubble radius and calculate the collapse pressure within the bubble. Ultrasound intensity has been selected as the control parameter to achieve the desired pressure from the bubble collapse. To find the minimum required pressure for clot fracture, the coupled blood and clot simulation has been calculated numerically according to the different initial pressures generated by the bubble collapse. In this solution, the collapse pressure amplitude is considered to be 1 MPa with a frequency of 5×10^{-7}. There is a clear correlation between clot stress and pressure pulse. Once the maximum pressure has been reached in the flow inlet, the amount of stress in the clot and its deformation will begin to change. There is no uniform distribution of pressure around the clot. There are two reasons for this: first of all, blood flows one way (upstream to downstream), which causes higher pressure at clot surfaces that are facing the flow direction. Accordingly, the opposite blood surface faces lower pressure. Secondly, this paper assumes the bubble is collapsing near one side of the clot. As a result, it exerts unsymmetrical pressure on the clot surface. This causes the clot to be removed by creating higher pressure on one side.

As part of thrombolysis, we need a pulse of pressure from the bubble collapse in order to fracture the clot. For simulating the behavior of the clot, different pressure values are applied to the clot surface due to different bubble collapses. Each input pressure is converted into equivalent stress on the clot surface.

According to reference [2], the Range of the deformation behavior of the specimens changes, meaning the yield stress in this case is between 4000 and 6000 Pa, which we consider equal to 4500 Pa, as shown in Fig. 9. Yield stress is the amount of stress that a material needs to be deformed. Comparison of the stress on the clot with the yield stress of the clot shows a minimum pressure pulse of 0.2 MPa needed for the deformation of the clot, which is the purpose of this paper. Now we can use Table 2 to get the optimal value for ultrasound intensity, which is equal to 1 $\frac{W}{cm^2}$.

The clot without any applied pressure is shown in Fig. 5. In Fig. 6 and Fig. 7, the clot deformation in mm with the max pressure pulse equal to 0.6 MPa and 0.2 MPa is shown, respectively. The main goal of the fluid analysis presented in this paper is to evaluate ability of the proposed approach for numerical analysis of the blood clot deformation using the ultrasound bubble control. The results indicate that we need a minimum pressure pulse of 0.2 MPa to deform the clot. It may not be enough for clot removal and may just deform it. In Fig. 8, the equivalent stress in MPa with the maximum pressure pulse=0.2 MPa is shown. It is noted that this research is the first step for clot removal using the bubble collapse, and completed studies will be presented in the future.

It should be mentioned that the compared yield stress is similar for all amounts of stress. As listed in Table 2, the minimum pressure required for deforming the blood clot can be reached by exerting an ultrasound with an intensity of 2 $\frac{W}{cm^2}$.

In Fig. 9, the aim of showing the different pressure pulses, including a pressure pulse of 0.6 MPa, is to investigate a large range of pressure pulses for comparing them with the yield stress. In fact, we want to show that with different amounts of pressure, in which way the clot will behave. In this way, we will have more precise investigations to prove the results.

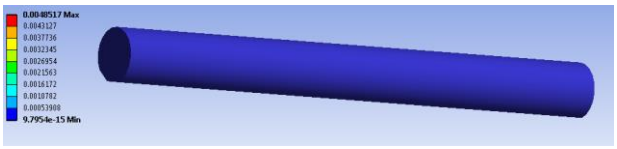

Fig. 5. Clot without pressure.

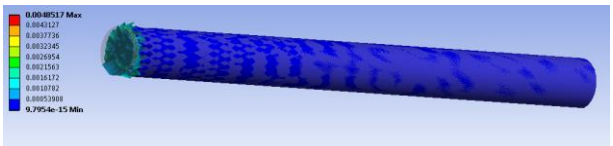

Fig. 6. Clot deformation(mm) with the max pressure pulse=0.6 MPa.

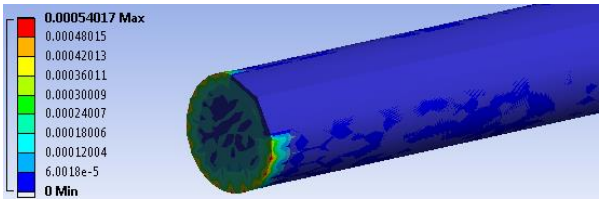

Fig. 7. Clot deformation(mm) with the max pressure pulse=0.2 MPa.

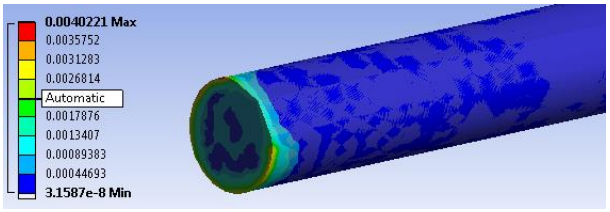

Fig. 8. Equivalent stress (Mpa) with the max pressure pulse=0.2 MPa.

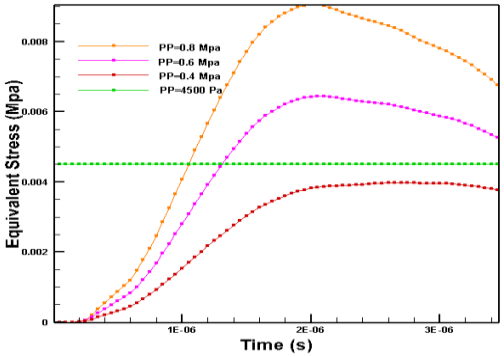

Fig. 9. Comparison of the equivalent stress on the clot in different pressure pulses with the amount of yield stress=4500 Pa.

6. CONCLUSIONS

A clot fracture requires a minimum pressure pulse from a bubble collapse during the thrombolysis process. The purpose of this paper is to discuss the solution of the RP equation, which determines the pressure resulting from the collapse of a single spherical bubble in blood. As a result of the numerical solution, the pressure created by bubble collapse varies with the driving ultrasound intensity. In this way, choosing an ultrasound intensity accurately for the intended pressure results in deforming the blood clot. According to the different initial pressures generated by bubble collapse, coupling blood and clot simulation has been numerically performed to find the minimum pressure required for clot deformation. To simulate different bubble collapses and clot behaviors, different pressures were applied to the clot surface. The equivalent stress and total deformation of the clot surface have been calculated for each input pressure. A comparison of the stress on the clot with the yield stress of the clot indicates that 0.6 MPa is the minimum pressure pulse required to pass the yield stress and have a deformation in the clot. This minimum pressure can be achieved by exerting an ultrasound with an intensity of $2\,W/(cm^2)$. The simulations confirmed the numerical results obtained. In the continuation of this research, the practical implementation of the proposed method with the obtained parameters is suggested.

CONFLICTS OF INTEREST

The authors declare that they have no conflict of interest.

REFERENCES

[1] WebMD Medical Reference Reviewed by James Beckerman, MD, FACC on March 21, 2019.

[2] F. Bajd and I. Serša, "Mathematical modeling of blood clot fragmentation during flow-mediated thrombolysis," *Biophysical journal*, vol. 104, no. 5, pp. 1181-1190, 2013.

[3] J. M. Wardlaw, V. Murray, E. Berge, and G. J. Del Zoppo, "Thrombolysis for acute ischaemic stroke," *Cochrane Database of Systematic Reviews* (7), 2014, https://doi.org/10.1002/14651858.CD000213.pub3.

[4] L. R. Wechsler, "Intravenous thrombolytic therapy for acute ischemic stroke," *the New England Journal of Medicine*, vol. 364, no. 22, pp. 2138–2146, 2011, https://doi.org/10.1056/NEJMct1007370.

[5] E. A. Mistry *et al*., "Mechanical thrombectomy outcomes with and without intravenous thrombolysis in stroke patients: A meta-analysis," *Stroke*, vol. 48, no. 9, pp. 2450–2456, 2017, https://doi.org/10.1161/STROKEAHA.117.017320.

[6] S. Z. Goldhaber, L. Visani, and M. De rosa, "Acute pulmonary embolism: Clinical outcomes in the international cooperative pulmonary embolism registry (ICOPEr)," *Lancet*, vol. 353, no. 9162, pp. 1386–1389, 1999.

[7] S. Z. Goldhaber *et al*., "Alteplase versus heparin in acute pulmonary embolism: Randomised trial assessing right ventricular function and pulmonary perfusion," *Lancet*, vol. 341, no. 8844, pp. 507–511, 1993, https://doi.org/10.1016/0140-6736(93)90274-K.

[8] K. Ouriel, F. J. Veith, and A. A. Sasahara, "A comparison of recombinant urokinase with vascular surgery as initial treatment for acute arterial occlusion of the legs," *the New England Journal of Medicine*, vol. 338, no. 16, pp. 1105–1111, 1998,

https://doi.org/10.1056/NEJM199804163381601.

[9] F. R. Young, *Cavitation*, London, UK: Imperial College Press, 1999.

[10] T. J. Mason, *Advances in Sonochemistry*, vol. 1–6, Amsterdam, The Netherlands: Elsevier, 1990–2001.

[11]K. S. Suslick, *Ultrasound: Its chemical, physical, and biological effects*, New York: VCH Publishers, 1988.

[12]R. k. Bhaskaracharya, S. Kentish, and M. Ashokkumar, "Selected applications of ultrasonics in food processing," *Food Engineering Reviews*, vol. 1, no. 1, pp. 31–49, 2009, https://doi.org/10.1007/s12393-009-9003-7.

[13]D. L. Miller *et al*., "Overview of therapeutic ultrasound applications and safety considerations," *Journal of Ultrasound in Medicine*, vol. 31, no. 4, pp. 623-634, 2012, https://doi.org/10.7863/jum.2012.31.4.623.

[14]U. B. Mahatme, M. Archana, S. P. Dongre, A. S. Nakhate, and A. V. Tabhane, "Applications of ultrasound in medical science: A review," in *International Symposium on Ultrasonics*, Nagpur, Maharashtra, India, 2015, pp. 134-144.

[15] F. R. Young, *Cavitation*, London: McGraw-Hill, 1994.

[16]Sh. Niazi, S. H. Hashemabadi, and M. Mirarab Razi, "CFD simulation of acoustic cavitation in a crude oil upgrading sonoreactor and prediction of collapse temperature and pressure of a cavitation bubble," *Chemical Engineering Research and Design*, vol. 92, no. 1, pp. 166-173, 2014, https://doi.org/10.1016/j.cherd.2013.07.002.

[17]S. Merouani, O. Hamdaoui, Y. Rezgui, and M. Guemini, "Theoretical estimation of the temperature and pressure within collapsing acoustical bubbles," *Ultrasonics Sonochemistry*, vol. 21, no. 1, pp. 53–59, 2014, https://doi.org/10.1016/j.ultsonch.2013.05.008.

[18]S. Li, R. Han, A. M. Zhang, and Q. X. Wang, "Analysis of pressure field generated by a collapsing bubble," *Ocean Engineering*, vol. 117, pp. 22-38, 2016, https://doi.org/10.1016/j.oceaneng.2016.03.016.

[19]K. Y. Kim, K. T. Byun, and H. Y. Kwak, "Temperature and pressure fields due to collapsing bubble under ultrasound," *Chemical Engineering Journal*, vol. 132, no. 1-3, pp. 125-135, 2007, https://doi.org/10.1016/j.cej.2007.01.037.

[20]J. M. Brett and A. Krelle, "A study of bubble collapse pressure pulse waves from small scale underwater explosions near the water surface," *Journal of Sound and Vibration*, vol. 435, pp. 91-103, 2018, https://doi.org/10.1016/j.jsv.2018.08.004.

[21]A. D. Maxwell, C. A. Cain, A. P. Duryea, L.Yuan, H. S. Gurm, and Z. Xu, "Non-invasive thrombolysis using pulsed ultrasound cavitation therapy-histotripsy," *Ultrasound in Medicine and Biology*, vol. 35, no. 12, pp. 1982–1994, 2009, https://doi.org/10.1016/j.ultrasmedbio.2009.07.001.

[22]Z. Xu, T. L. Hall, J. B. Fowlkes, and C. A. Cain, "Effects of acoustic parameters on bubble cloud dynamics in ultrasound tissue erosion (histotripsy)," *Journal of Acoustical Society of America*, vol. 122, pp. 229–236, 2007, https://doi.org/10.1121/1.2735110.

[23]Z. Hormozi Moghaddam, M. Mokhtari Dizaji, M. Movahedin, and M. E. Ravari, "Estimation of the distribution of low-intensity ultrasound mechanical index as a parameter affecting the proliferation of spermatogonia stem cells in vitro," *Ultrasonics Sonochemistry*, vol. 37, pp. 571-581, 2017, https://doi.org/10.1016/j.ultsonch.2017.02.013.

[24]M. Najafi, R. Kamali Moghadam, M. Azadegan, N. Sahranavard Fard, and M. Mohammadi, "Ultrasound bubble control for blood clot deformation in a vessel connected to a pulmonary artery," in *American Control Conference (ACC)*, New Orleans, LA, USA, 2021, pp. 1464-1469, https://doi.org/10.23919/ACC50511.2021.9482904.

[25]M. Mobasheri, M. Mokhtari Dizaji, T. Toliyat, and M. Mehrpour, "Destruction of recombinant tissue plasminogen activator (rtPA) -loaded echogenic liposomes under dual frequency sonication," *Journal of Kerman University of Medical Sciences*, vol. 25, no. 3, pp. 243-254, 2018.

[26]M. Najafi, M. Azadegan, and M. T. Beheshti, "Stability analysis and sliding mode control of a single spherical bubble dynamics," In *American Control Conference (ACC)*, Boston, MA, USA, 2016, pp. 5050-5055, https://doi.org/10.1109/ACC.2016.7526154.

[27]Y. T. Shah, A. B. Pandit, and V. S. Moholkar, *Cavitation Reaction Engineering*, New York, N.Y.: Kluwer Academic/Plenum Publishers, 1999, P. 23.

[28]E. A. Brujan, "Collapse of cavitation bubbles in blood," *Europhysics Letters*, vol. 50, no. 2, pp. 175–181, 2000, https://doi.org/10.1209/epl/i2000-00251-7.

[29]I. V. Pivkin, P. D. Richardson, and G. Karniadakis, "Blood flow velocity effects and role of activation delay time on growth and form of platelet thrombi," *National Academy of Sciences of the United States of America*, vol. 103, no. 46, pp. 17164-17169, 2006, https://doi.org/10.1073/pnas.0608546103.

[30]S. L. Diamond, "Systems biology to predict blood function," *Journal of Thrombosis and Haemostasis*, vol. 7, pp. 177–180, 2009, https://doi.org/10.1111/j.1538-7836.2009.03463.x.

[31]W. P. Jones and B. E. Launder, "The prediction of laminarization with a two-equation model of turbulence," *International Journal of Heat and Mass Transfer*, vol. 15, no. 2, pp. 301-314, 1972, https://doi.org/10.1016/0017-9310(72)90076-2.

[32]B. E. Launder and B. I. Sharma, "Application of the energy dissipation model of turbulence to the calculation of flow near a spinning disc," *Letters in Heat and Mass Transfer*, vol. 1, no. 2, pp. 131-137, 1974, https://doi.org/10.1016/0094-4548(74)90150-7.

[33] J. E. Bardina, P. G. Huang, and T. J. Coakley, "Turbulence modeling validation, testing, and development," NASA, Tech. Memorandum, 110446, 1997.

[34]P. C. Kohnke, *Ansys Theory References, Release 5.6*, 11rd ed. ANSYS Incorporated, 1999.